PHYSICAL REVIEW D VOLUME 27, NUMBER 7 1 APRIL 1983

Constituent-quark model for production of forward hyperons in proton-nucleus collisions

Fujio Takagi
Department of Physics, Tohoku University, Sendai 980, Japan
(Received 8 September 1982)

Cross sections for the inclusive reactions $p+A\to\Lambda$ or Ξ^0+anything in the proton fragmentation region are analyzed in terms of the constituent-quark model. Contributions from the leading single quarks and leading diquarks are determined separately and the results are interpreted in terms of the quark-fragmentation-recombination picture. It is strongly suggested that recombination of leading quarks with a heavy (anti)quark ($s,\bar{s},c,\bar{c},\ldots$) or a pair of (anti)quarks from the central sea is strongly suppressed compared to recombination with a single light (anti)quark (u, $\bar{u}$, d, or $\bar{d}$) from the sea.

I. INTRODUCTION

It is now widely recognized that both hadrons and nuclei are equally useful to study strong interactions at high energies in terms of hadronic constituents, i.e., quarks and gluons. In particular, the notion of constituent quarks with the quark additivity approximation for hadron-hadron (hh) collisions has been shown to be very useful to describe not only hh collisions but also hadron-nucleus (hA) [and probably nucleus-nucleus (AA)] collisions at high energies. The most successful case in hA collisions is found in the application to the projectile fragmentation region.[1-7]

Experimentally, inclusive single-particle spectra in reactions $h+A\to c+$anything show a distinct effect of nuclear attenuation in the forward region. That is, the yield of a hadron c in the projectile fragmentation region decreases as the mass number A increases. In order to describe the A dependence, experimentalists conventionally parametrize the cross sections in the form

$$f_{hA}^c(x,p_T)=\eta_h^c(x,p_T)\exp[\alpha_h^c(x,p_T)\ln A] \tag{1.1a}$$

or

$$g_{hA}^c(x)=\zeta_h^c(x)\exp[\alpha_h^c(x)\ln A]\ , \tag{1.1b}$$

where

$$f_{hA}^c(x,p_T)\equiv E\frac{d^3\sigma(hA\to cX)}{d^3\vec{p}} \tag{1.2a}$$

and

$$g_{hA}^c(x)\equiv\int dp_T{}^2 f_{hA}^c(x,p_T)\ . \tag{1.2b}$$

If one parametrizes also the A dependence of cross sections for nondiffractive inelastic h-A collisions by the power law

$$\sigma_{hA}=\sigma_h^0\exp(\alpha_h^0\ln A)\ , \tag{1.3}$$

then the nuclear attenuation implies that

$$\alpha_h^c(x)\text{ or }\alpha_h^c(x,p_T)<\alpha_h^0\ , \tag{1.4}$$

for a certain range of x and p_T.

All the hitherto measured reactions exhibit a clear attenuation effect that depends rather strongly on the reaction mode $h\to c$. Some salient features are the following.[8-10] (i) Both pion fragmentation into charged mesons $c=\pi^\pm$, $K^\pm$ and proton fragmentation into $\pi^\pm$ show a rather x-independent attenuation, i.e.,

$$\alpha_\pi^0-\alpha_\pi^c(x,p_T)\simeq\alpha_p^0-\alpha_p^\pi(x,p_T)\simeq 0.12\text{–}0.13$$

for $0.3\lesssim x\lesssim 0.9$. (ii) Proton fragmentation into p or Λ exhibit an x-dependent strong attenuation, i.e.,

$$\alpha_p^p(x,p_T)\simeq\alpha_p^\Lambda(x,p_T)<\alpha_p^0$$

for $0.2\lesssim x\lesssim 0.9$ and small p_T, both $\alpha_p^p(x,p_T)$ and $\alpha_p^\Lambda(x,p_T)$ decreases monotonically as x increases and

$$\alpha_p^0-\alpha_p^B(x,p_T)\simeq 0.21$$

for $x\gtrsim 0.9$ and $B=p$ and Λ. To my knowledge, the constituent-quark model (CQM) first applied to hA collisions by Anisovich *et al.*[1] and, later on, developed further by many people[2-7] is the only model that can explain simultaneously the above features (i) and (ii). However, the uncertainties of

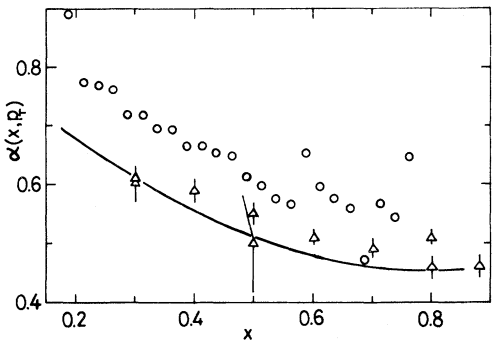

FIG. 1. The observed values of the exponent $\alpha_p^B(x,p_T)$ for $B=p$ ($p_T=0.3$ and 0.5 GeV/c, open triangles), $B=\Lambda$ ($p_T=0$ GeV/c, solid curve), and $B=\Xi^0$ ($p_T\simeq 0$ GeV/c, open circles). Error bars of Ξ^0 data points are not shown.

experimental data are so large that one cannot rule out other models at present.

Recently, experimental data with high precision have been obtained for the reaction

$$p+A\to\Xi^0+\text{anything} \tag{1.5}$$

at 300 GeV/c.[11] The data show again a clear attenuation effect which is, however, clearly different from the one seen in $pA\to pX$ (Ref. 10) or $pA\to\Lambda X$.[8,9] See Fig. 1 for experimental values of $\alpha_p^B(x,p_T)$ for $B=p$, Λ, and Ξ^0. The attenuation in $pA\to\Xi^0X$ is definitely weaker than that in the other reactions, i.e.,

$$\alpha_p^{\Xi^0}(x,p_T)>\alpha_p^B(x,p_T)\quad (B=p \text{ or } \Lambda)$$

for the whole range of x. Hence, we consider it worthwhile to analyze the reaction $pA\to\Xi^0X$ together with $pA\to\Lambda X$ (Ref. 9) in terms of the CQM. Although a similar analysis has already been carried out for $pA\to\Lambda X$ by Białas *et al.*[4] and by Berlad *et al.*,[5] our results show an important difference from those in Ref. 4 as will be discussed in Sec. III. The procedure of analysis adopted in Ref. 5 is different from ours.

This paper is organized as follows. General formalism is given in Sec. II. Reactions $pA\to\Lambda X$ and $pA\to\Xi^0X$ are analyzed in Secs. III and IV, respectively. An interpretation of the results in terms of a quark-fragmentation-recombination picture is given in Sec. V. Section VI is devoted to discussions and conclusions.

II. GENERAL FORMALISM

Consider an inclusive reaction

$$p+A\to B+\text{anything , for } B=\text{a baryon ,}$$

in the projectile (proton) fragmentation region. According to the CQM, the cross section is expressed as

$$g_{pA}^B(x)/\sigma_{pA}=P_{pA}^{(1)}g_{p\to B}^{(1)}(x)+P_{pA}^{(2)}g_{p\to B}^{(2)}(x)\ , \tag{2.1}$$

where $P_{pA}^{(i)}$ is the probability that i constituent quarks out of three in an incident proton make inelastic collisions with a target nucleus, and $g_{p\to B}^{(i)}(x)$ is the x distribution of baryons B that come from fragmentation or recombination of the corresponding leading quarks. The other cross sections $f_{pA}^B(x,p_T)$ can be expressed similarly. Contributions from the wounded quarks for $x\gtrsim 0.2$ are assumed to be negligible.[4,5,12] The situation is illustrated in Fig. 2. The explicit form of the probabilities $P_{pA}^{(i)}$ is

$$\begin{aligned} P_{pA}^{(1)}&=3(\sigma_{pA}-\sigma_{\pi A})/\sigma_{pA}\ ,\\ P_{pA}^{(2)}&=3(2\sigma_{\pi A}-\sigma_{pA}-\sigma_{qA})/\sigma_{pA}\ ,\\ P_{pA}^{(3)}&=1-P_{pA}^{(1)}-P_{pA}^{(2)}\ , \end{aligned} \tag{2.2}$$

where σ_{pA}, $\sigma_{\pi A}$, and σ_{qA} are inelastic pA, πA, and qA cross sections, respectively. A crucial point here is the fact that $P_{pA}^{(1)}$ decreases monotonically while both $P_{pA}^{(2)}$ and $P_{pA}^{(3)}$ increase monotonically as A increases up to $A\simeq 240$. If the cross section $g_{pA}^B(x)$ is dominated by diagram 2(a), then the spectrum should show a strong nuclear attenuation because of the A dependence of $P_{pA}^{(1)}$. As diagram 2(b) gets important relative to diagram 2(a), the attenuation becomes weaker because the A dependence of $P_{pA}^{(2)}$ cancels partially that of $P_{pA}^{(1)}$. As will be discussed in more detail in Sec. V, this is the general reason why the attenuation in $pA\to\Xi^0X$ is weaker than that in $pA\to\Lambda X$.

Before analyzing the experimental data by using (2.1), one has to choose a set of cross sections σ_{pA}, $\sigma_{\pi A}$, and σ_{qA}. For σ_{pA} and $\sigma_{\pi A}$, we use

$$\sigma_{pA}=44.9A^{0.695}\text{ mb}\ , \tag{2.3a}$$

$$\sigma_{\pi A}=28.5A^{0.752}\text{ mb}\ , \tag{2.3b}$$

which are the best power-law fits to the average

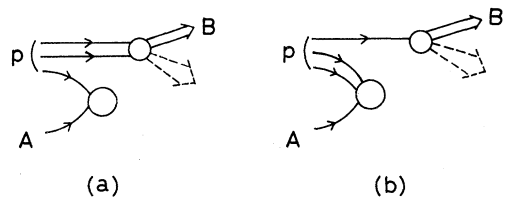

FIG. 2. In pA collisions, baryons B in the fragmentation region of incident protons are produced through fragmentation or recombination of leading diquarks (a) or leading single quarks (b). The distributions $g_{p\to B}^{(1)}(x)$ and $g_{p\to B}^{(2)}(x)$ correspond to diagrams (a) and (b), respectively.

TABLE I. Inelastic cross sections σ_{pA} and quark absorption probabilities $P_{pA}^{(i)}$.

	Our parameters			Parameters used in Ref. 4			Experimental cross sections	
A	σ_{pA} (mb)[a]	$P_{pA}^{(1)}$	$P_{pA}^{(2)}$	σ_{pA} (mb)	$P_{pA}^{(1)}$	$P_{pA}^{(2)}$	σ_{pA} (mb)[b]	σ_{pA} (mb)[c]
Be	206.8	0.846	0.146	194.2	0.738	0.229	210±2	
Cu	808.1	0.585	0.347	748.7	0.429	0.357	796±8	769±23
Pb	1827.8	0.421	0.432	1651.2	0.284	0.330	1812±35	1752±53

[a]A smooth fit given by (2.3a) to the cross sections averaged over $E=20$–60 GeV from Ref. 13.

[b]Cross sections averaged over $E=20$–60 GeV from Ref. 13.

[c]Cross sections at $E=280$ GeV from Ref. 14.

cross sections measured by Denisov *et al.* for the incident energies 20–60 GeV.[13] In order to estimate σ_{qA}, we use a standard optical geometrical formula at the constituent-quark level, assume the quark additivity in hadron- (or quark-) nucleon collisions, and use for simplicity the uniform-disk approximation for quark densities in nuclei. The cross sections for inelastic iA collisions (here, $i=$a hadron or a quark) are then given as

$$\sigma_{iA}=\pi b_A^{\,2}\left[1-\left[1-\frac{\text{“}\sigma_{qq}\text{”}}{\pi b_A^{\,2}}\right]^{3AC_i}\right], \tag{2.4}$$

where b_A is the radius of the nuclear disk, “σ_{qq}” is the effective qq cross section, and C_i is the number of constitutent (anti)quarks contained in a particle i, and hence $C_p=3$, $C_\pi=2$, and $C_q=1$. We first reproduce the “experimental” cross sections given by (2.3a) and (2.3b) by freely adjusting the values of b_A and “σ_{qq}” for individual A. The cross sections σ_{qA} are then calculated by simply putting $C_i=1$ in (2.4). The effective cross section “σ_{qq}” turns out to be slightly dependent on A. This is an indication that the uniform disk approximation is not very accurate. Nevertheless, we believe that the above procedure is not too bad as a method of extrapolation

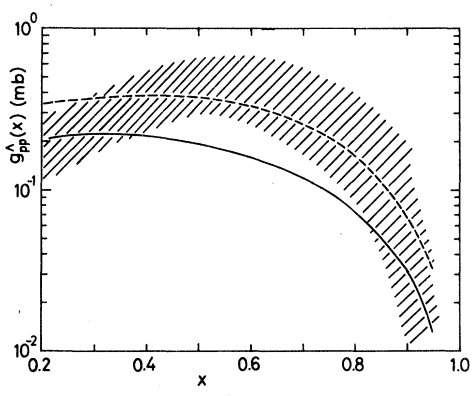

FIG. 3. The solid curve represents the CQM extrapolation of $g_{pA}^{\Lambda}(x)$ to $A=1$. Experimental data on $g_{pp}^{\Lambda}(x)$ are shown by the shaded region. The dashed curve is the A^α extrapolation from Be and Pb data to $A=1$.

from the points where $C_i=3$ and 2 to the point where $C_i=1$.

Our choices of σ_{pA} and $P_{pA}^{(i)}$ are listed in Table I for three kinds of nuclei, where the same quantities used in Ref. 4 as well as two sets of experimental σ_{pA} from two groups[13,14] are also shown for comparison. Note a significant difference between our parameters and those used in Ref. 4. Now we are ready to determine $g_{p\to B}^{(i)}(x)$ [or $f_{p\to B}^{(i)}(x,p_T)$] by comparing (2.1) with experimental data.

III. $p+A\to\Lambda+$anything

We have calculated the experimental cross sections $g_{pA}^{\Lambda}(x)$ by integrating $f_{pA}^{\Lambda}(x,p_T)$ given in Table VI of Ref. 9 over $p_T{}^2$. The data are available for $A=$Be and Pb at incident proton energy 300 GeV. Since two unknown functions $g_{p\to\Lambda}^{(i)}(x)$ $(i=1,2)$ are involved in (2.1), they can be determined by using the two experimental cross sections $g_{pA}^{\Lambda}(x)$ for $A=$Be and Pb as inputs. The result for $g_{p\to\Lambda}^{(i)}(x)$ parametrized in the form $cx^a(1-x)^b$ is

$$g_{p\to\Lambda}^{(1)}(x)=0.0265x^{0.622}(1-x)^{1.349}, \tag{3.1a}$$

$$g_{p\to\Lambda}^{(2)}(x)=0.0594(1-x)^{4.5}, \tag{3.1b}$$

both for $0.2\lesssim x\lesssim 0.85$. Here, the uncertainty of $g_{p\to\Lambda}^{(1)}(x)$ for $0.2\lesssim x\lesssim 0.85$ and that of $g_{p\to\Lambda}^{(2)}(x)$ for $0.2\lesssim x\lesssim 0.7$ are comparable to that of the input $g_{pA}^{\Lambda}(x)$, i.e., well less than 10%. However, the uncertainty of $g_{p\to\Lambda}^{(2)}(x)$ for $0.75\lesssim x$ is so large that any smooth extrapolation from smaller x is possible as long as it is positive and decreases monotonically as x increases.

From (3.1a) and (3.1b), one obtains the cross section for the reaction $p+p\to\Lambda+$anything:

$$g_{pp}^{\Lambda}(x)=\sigma_{pp}g_{p\to\Lambda}^{(1)}(x), \tag{3.2}$$

where the quark-additivity approximation, $P_{pp}^{(1)}=1$ and $P_{pp}^{(2)}=0$, has been used. This is a model-dependent extrapolation of $g_{pA}^{\Lambda}(x)$ to $A=1$. In Fig. 3, the extrapolated cross section calculated from (3.1a) and (3.2) with $\sigma_{pp}=28.5$ mb is compared with

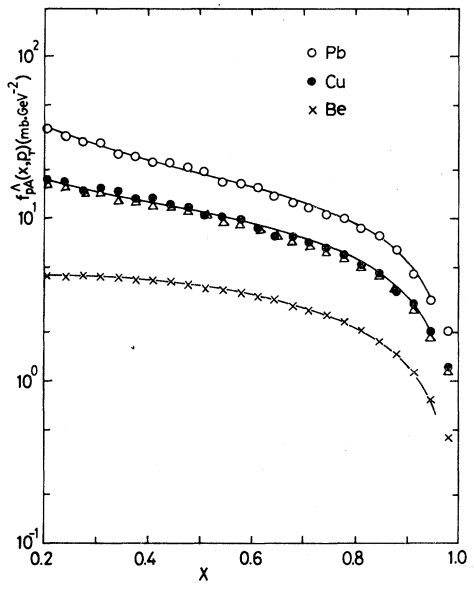

FIG. 4. The cross sections $f^{\Lambda}_{pA}(x,p_T=0)$ calculated from (3.3a) and (3.3b) are shown by the solid curves in comparison with the experimental data (Ref. 9). Actually, the curves for Be and Pb are our CQM fit while the curve for Cu is the CQM interpolation. The open triangles are the A^{α} interpolation from Be and Pb data points to Cu.

data on $pp\to\Lambda X$.[15–17] The agreement is satisfactory though not perfect. For comparison, the result of an extrapolation by using the power-law fit (1.1b) is also shown there.

A similar analysis was carried out for the cross sections measured at $\theta_{\rm lab}=0.25$ mrad.[9] Since the p_T dependence at a given x is very weak at small p_T, the cross sections for such a small angle can be approximately regarded as $f^{\Lambda}_{pA}(x,p_T)$ for $p_T\simeq 0$. The result obtained by using pBe and pPb data is

$$f^{(1)}_{p\to\Lambda}(x,0)=0.0532x^{0.456}(1-x)^{0.858}\ (\mathrm{GeV}/c)^{-2}\ , \tag{3.3a}$$

$$f^{(2)}_{p\to\Lambda}(x,0)=0.070(1-x)^{4.5}\ (\mathrm{GeV}/c)^{-2}\ , \tag{3.3b}$$

both for $0.2\lesssim x\lesssim 0.95$. Again the uncertainty of $f^{(2)}_{p\to\Lambda}(x,0)$ is large for $0.65\lesssim x$. The cross sections reproduced for $A=$Be and Pb, or interpolated to $A=$Cu by using (3.3a) and (3.3b) are shown in Fig. 4 together with the experimental data.[9] Another interpolation to $A=$Cu by assuming A^{α} behavior is also shown for comparison. Agreement of our CQM interpolation with pCu data is better than that of the A^{α} interpolation.

As was mentioned in Sec. I, the same data were analyzed by A. Białas and E. Białas.[4] Our result for $f^{(1)}_{p\to\Lambda}(x,0)$ [Eq. (3.3a)] is consistent with theirs. There is, however, a big discrepancy as to the result on $f^{(2)}_{p\to\Lambda}(x,0)$. Their $f^{(2)}_{p\to\Lambda}(x,0)$ is so hard that it behaves like $(1-x)^{1.5}$ at large x. A main cause of the discrepancy is identified with the different sets of cross sections (and hence the probability $P^{(2)}_{pA}$) used in the two analyses. See Table I. Note that the cross sections σ_{pA} used in Ref. 4 are not consistent (at least, not in good agreement) with either experimental cross sections of Ref. 13 or of Ref. 14.

IV. $p+A\to\Xi^0+$anything

By following the same procedure as was described in the preceding section, the fragmentation functions of incident protons into Ξ^0 via leading quarks are determined from the data on $pA\to\Xi^0X$ for $A=$Be, Cu, and Pb.[11] Actually, the fragmentation functions $f^{(i)}_{p\to\Xi^0}(x,0)$ are overdetermined if one uses all the data on three kinds of nuclei at the same time. So we have first calculated them in three ways by using Be and Cu data, or Be and Pb data, or Cu and Pb data. Although some points of the three sets of $f^{(i)}_{p\to\Xi^0}(x,0)$ thus calculated show large fluctuations for some x (mainly for $x\gtrsim 0.6$) due to fluctuations of the corresponding data points, other points have reasonably small fluctuations around the averages of the three sets. That is, the deviations from the averages, of about 60% (75%) of all the calculated values of $f^{(i)}_{p\to\Xi^0}(x,0)$ are well less than $\pm 30\%$ ($\pm 50\%$). So we have simply taken the average of the three sets and then made a smooth fit by using a functional form constant $\times(1-x)^{a}$. The final result is

$$f^{(1)}_{p\to\Xi^0}(x,0)=0.001\,09(1-x)^{2.5}\ (\mathrm{GeV}/c)^{-2}\ , \tag{4.1a}$$

$$f^{(2)}_{p\to\Xi^0}(x,0)=0.003\,52(1-x)^{4.5}\ (\mathrm{GeV}/c)^{-2}\ , \tag{4.1b}$$

both for $0.2\lesssim x\lesssim 0.8$. However, the uncertainty of $f^{(2)}_{p\to\Xi^0}(x,0)$ is very large for $0.6\lesssim x$. The cross sections reproduced from (4.1a) and (4.1b) are shown in Fig. 5 with the experimental data.[11].

V. INTERPRETATION IN TERMS OF QUARK FRAGMENTATION-RECOMBINATION

We would like to interpret the results on $f^{(i)}_{p\to B}(x,0)$ [or $g^{(i)}_{p\to B}(x)$] for $B=\Lambda$ and Ξ^0 obtained in Secs. III and IV in terms of CQM with fragmentation or recombination of leading quarks. In the original model proposed by Anisovich *et al.*,[1] a hadron in the projectile fragmentation region is produced via "pure" recombination of leading quarks with (anti)quarks with small momentum in the cen-

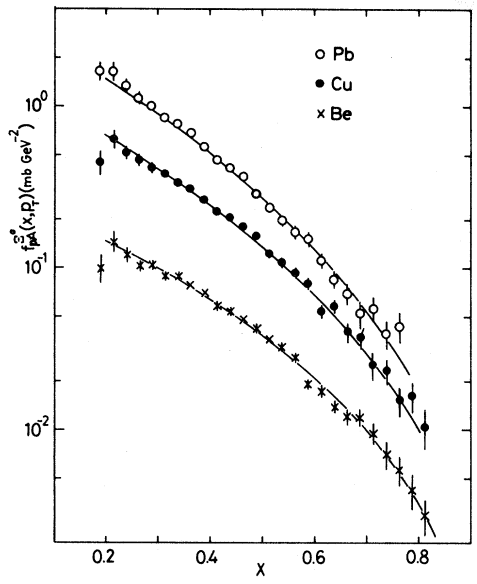

FIG. 5. The cross sections $f^{\Xi^0}_{pA}(x,p_T=0)$ calculated from (4.1a) and (4.1b) are shown by the solid curves in comparison with the experimental data (Ref. 11).

tral sea. The main mechanisms which contribute to $g^{(1)}_{p\to\Lambda}(x)$ [or $f^{(1)}_{p\to\Lambda}(x,p_T)$] and $g^{(2)}_{p\to\Lambda}(x)$ [or $f^{(2)}_{p\to\Lambda}(x,p_T)$] would then be given by the diagrams shown in Figs. 6(a) and 6(b), respectively. (Such an annoying twofold expression as $g^{(i)}_{p\to B}(x)$ [or $f^{(i)}_{p\to B}(x,p_T)$] will not be repeated hereafter, and hence the twofold meaning, when relevant, is to be understood.) A smearing effect due to resonance production and their decay is to be understood hereafter. The exponent of $1-x$ [1.349 in $g^{(1)}_{p\to\Lambda}(x)$ and 4.5 in $g^{(2)}_{p\to\Lambda}(x)$] seems, however, too large for those diagrams being dominant. In fact, if one admits that the reaction $pp\to\Lambda X$ is dominated by the diagram that corresponds to the one shown in Fig. 6(a), one would fall into a difficulty in explaining the different shapes of x distributions of $pp\to\Lambda X$ and $pp\to nX$.[18] Hence, we would like to suggest that the

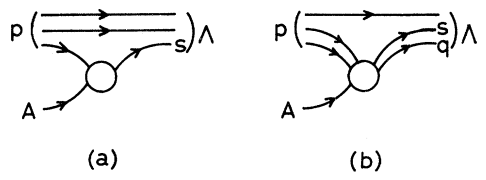

FIG. 6. Production of Λ in the incident proton fragmentation region in pA collisions would be dominated by diagrams (a) or (b) if "pure" recombination of leading quarks were responsible for it. Here, $q=u$ or d. Actually, contributions from those diagrams will be strongly suppressed because a heavy quark or a pair of quarks have to be picked up from the central sea.

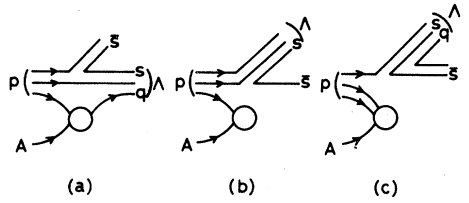

FIG. 7. The diagrams that will actually give the main contribution to production of Λ in the proton fragmentation region in pA collisions. Here, q is a light quark, i.e., u or d. Those diagrams are free from the suppression mechanism discussed in the text and in Ref. 18.

reaction $pA\to\Lambda X$ is dominated by the diagrams shown in Fig. 7. The rules here are the following[18]: (i) Recombination of a leading quark with a heavy (anti)quark ($s,\bar{s},c,\bar{c},b,\bar{b},\ldots$) from the central sea is strongly suppressed compared to recombination with a light (anti)quark (u, $\bar{u}$, d, or $\bar{d}$) from the sea. (ii) Recombination of a leading quark with a pair of (anti)quarks from the sea is likewise suppressed compared to recombination with a light (anti)quark from the sea. This suppression mechanism is easily understood in terms of old-fashioned perturbation theory.[18]

One might wonder here if the diagram shown in Fig. 7(b) is really different from the one shown in Fig. 6(a). This point is related to the problem of possible equivalence between the recombination [e.g., Fig. 6(a)] and the fragmentation [e.g., Fig. 7(b)]. Our viewpoint is that they are not equivalent. This point may be most clearly explained by considering the x distributions of the Λ hyperons and the associated $\bar{s}$ quarks. In Fig. 6(a), the associated $\bar{s}$ quark in the central region (not shown explicitly) has a small x (it can be nearly vanishing) while the x of Λ is the sum of those of the leading diquark and the picked-up s quark. In Fig. 7(b), on the other hand, the diquark from the incident proton fragments into Λ and $\bar{s}$ in a scale-invariant way. Therefore, the x of Λ is, in general, smaller than that of the incident diquark in contrast with the recombination case of Fig. 6(a), and the $\bar{s}$ quarks have a nontrivial x distribution that can be entirely different from that of the $\bar{s}$ quarks in Fig. 6(a). In other words, the momentum of the leading diquark flows partially into the $\bar{s}$ quark in Fig. 7(b) while it does not in Fig. 6(a). This difference between Figs. 6(a) and 7(b) is indeed crucial in explaining the different x distributions of the reactions $pp\to\Lambda X$ and $pp\to nX$.[18]

For $p\to\Xi^0$, the model of Ref. 1 would suggest the diagrams shown in Figs. 8(a) and 8(b) as dominant processes for $f^{(1)}_{p\to\Xi^0}(x,p_T)$ and $f^{(2)}_{p\to\Xi^0}(x,p_T)$, respectively. The model would then predict that

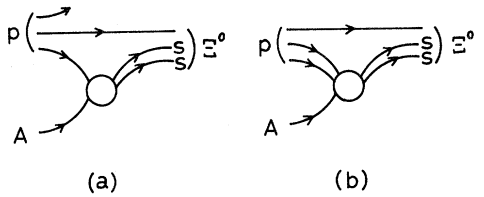

FIG. 8. Production of Ξ^0 in the proton fragmentation region would be dominated by diagrams (a) or (b) if "pure" recombination were responsible for it. Actually, those diagrams will be doubly suppressed because a pair of heavy quarks (ss) has to be picked up from the central sea.

$f^{(2)}_{p\to\Xi^0}(x,p_T)/f^{(1)}_{p\to\Xi^0}(x,p_T)$ is independent of x because the momentum flows from the leading quarks to the produced Ξ^0 in the two diagrams have the same structure. This is totally in disagreement with our result (4.1a) and (4.1b). If the suppression mechanisms (i) and (ii) operate actually, the diagrams shown in Fig. 9 will become dominant. Now the values of exponents of $1-x$ in our result [2.5 in $f^{(1)}_{p\to\Xi^0}(x,0)$ and 4.5 in $f^{(2)}_{p\to\Xi^0}(x,0)$] are quite reasonable. In Fig. 7(a), one strange meson must be emitted prior to recombination of a leading diquark into Λ. The x distribution of Λ from Fig. 7(b) is expected to be similar to or even slightly harder than that of Λ from Fig. 7(a). On the other hand, two strange mesons must be emitted prior to recombination of a leading diquark into Ξ^0. See Fig. 9(a). Therefore, the exponent of $f^{(1)}_{p\to\Xi^0}(x,p_T)$ should be larger than that of $f^{(1)}_{p\to\Lambda}(x,p_T)$. On the other hand, both diagrams shown in Figs. 7(c) and 9(b) have the same structure with respect to the momentum flow of leading quarks into Λ or Ξ^0. Hence, the exponent of $f^{(2)}_{p\to\Lambda}(x,p_T)$ must be the same as (at least similar to) that of $f^{(2)}_{p\to\Xi^0}(x,p_T)$. Both expectations are indeed the case in our results.

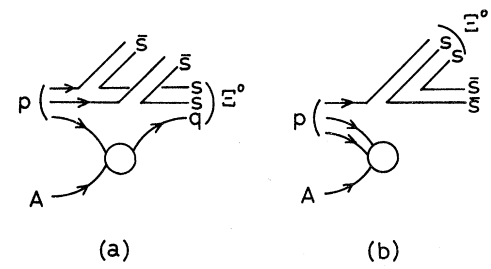

FIG. 9. The diagrams that will actually give the main contribution to production of Ξ^0 in the proton fragmentation region in pA collisions. Here, q is a light quark, i.e., u or d.

Finally, we would like to discuss the relative magnitudes between $f^{(1)}_{p\to B}(x,p_T)$ and $f^{(2)}_{p\to B}(x,p_T)$ for $B=\Lambda$ and Ξ^0. In order to produce Λ, one $s\bar{s}$ pair must be produced commonly in every diagram in Fig. 7. Similarly, two $s\bar{s}$ pairs must be produced in order to produce Ξ^0 in every diagram in Fig. 9. Therefore, the suppression factor for $s\bar{s}$ pair production relative to $u\bar{u}$ or $d\bar{d}$ production will be at least approximately canceled by taking the ratio $f^{(2)}_{p\to B}(x,p_T)/f^{(1)}_{p\to B}(x,p_T)$. Figure 7(c) is identical to Fig. 9(b) except for the flavor content of the produced quark-antiquark pairs, while the number of mesons emitted in Fig. 9(a) is larger than that in Fig. 7(a). Furthermore, there is an additional diagram Fig. 7(b) which contributes to $f^{(1)}_{p\to\Lambda}(x,p_T)$. Hence we expect that

$$f^{(2)}_{p\to\Xi^0}(x,p_T)/f^{(1)}_{p\to\Xi^0}(x,p_T) > f^{(2)}_{p\to\Lambda}(x,p_T)/f^{(1)}_{p\to\Lambda}(x,p_T)\,. \quad (5.1)$$

This inequality is the reason why the attenuation in $p\to\Xi^0$ is weaker than that in $p\to\Lambda$, and it is of course realized in our results (3.3a) and (3.3b) and (4.1a) and (4.1b).

VI. DISCUSSIONS AND CONCLUSIONS

Before concluding, we would like to mention an interesting observation made recently by Busza.[19] Compiling world data on pA collisions, he claims that $\alpha^c_p(x,p_T)$ is independent of c for $c=\pi^{\pm}$, K^0, K^+, p, n, and Λ within experimental uncertainties. If this universality were indeed the case for any c, all the existing models might be ruled out as was pointed out by him. However, we would like to point out two experimental facts which do not apparently reconcile with the suggested universality. (i) $\alpha^{\pi^+}_p(x,p_T)$ from Ref. 10 shows a significant deviation from the suggested universal curve. (ii) $\alpha^{\Xi^0}_p(x,p_T)$ from Ref. 11 is obviously different from $\alpha^{\Lambda}_p(x,p_T)$ from the same experimental group.[8,9] This is nothing but the reflection from the fact that the nuclear attenuation in $p\to\Xi^0$ is weaker than that in $p\to\Lambda$, one of the main points of this paper which are discussed at length. Therefore, it appears that the universality does not necessarily hold. However, we are also aware of another experimental fact that $\alpha^{K^0}_p(x,p_T)$ from Refs. 8 and 9 is very similar to $\alpha^{\Lambda}_p(x,p_T)$ in accordance with the universality. Such a similarity is not necessarily expected from CQM. A rather complicated mechanism may be necessary to explain it. Unfortunately, statistics of K^0 data are not so good as that of Λ or Ξ^0 data. So, we would like to urge experimentalists to provide K^0

data with higher statistics and wider x ranges. Better data are also needed for production of other particles such as $\pi^{\pm}$ and $K^{\pm}$ to prove (or disprove) the possible (but probably partial) universality of $\alpha_p^c(x,p_T)$. Of course, it is very interesting to measure further reactions such as $pA \to cX$ with $c = \phi, \rho^{\pm,0}, \omega, K^*, D, \ldots$.

To conclude, experimental data on the reactions $p + A \to \Lambda$ or Ξ^0 + anything in the proton fragmentation region are well explained in terms of the CQM if one assumes that recombination of a leading quark with a heavy (anti)quark or a pair of (anti)quarks from the central region is suppressed compared to recombination with a single light (anti)quark.

ACKNOWLEDGMENT

The author would like to thank L. G. Pondrom for providing him data on $p + A \to \Xi^0$ + anything prior to publication.

[1]V. V. Anisovich, Yu. M. Shabelski, and V. M. Shekhter, Nucl. Phys. B133, 477 (1978).
[2]N. N. Nikolaev and S. Pokorski, Phys. Lett. 80B, 290 (1979).
[3]A. Dar and F. Takagi, Phys. Rev. Lett. 44, 768 (1980).
[4]A. Białas and E. Białas, Phys. Rev. D 20, 2854 (1979).
[5]G. Berlad, A. Dar, and G. Eilam, Phys. Rev. D 22, 1547 (1980).
[6]F. Takagi, Prog. Theor. Phys. 65, 1350 (1981).
[7]A. Białas and W. Czyz, Nucl. Phys. B194, 21 (1982).
[8]K. Heller *et al.*, Phys. Rev. D 16, 2737 (1977).
[9]P. Skubic *et al.*, Phys. Rev. D 18, 3115 (1978).
[10]A. E. Brenner *et al.*, Report No. Fermilab-Conf-80/47-Exp., submitted to XXth International Conference High Energy Physics, Madison, Wisconsin, 1980 (unpublished).
[11]L. G. Pondrom *et al.*, in *Proceedings of the Xth International Symposium on Multiparticle Dynamics, Goa, India, 1979,* edited by S. N. Ganguli, P. K. Malhotra, and A. Subramanian (Tata Institute, Bombay, 1980), p. 579; L. G. Pondrom (private communication).
[12]G. Berlad and A. Dar, Israel Institute of Technology Report No. TECHNION-PH-79-69, 1979 (unpublished).
[13]S. P. Denisov *et al.*, Nucl. Phys. B61, 62 (1973).
[14]A. S. Carroll *et al.*, Phys. Lett. 80B, 319 (1979).
[15]J. W. Chapman *et al.*, Phys. Lett. 47B, 465 (1973).
[16]A. Sheng *et al.*, Phys. Rev. D 11, 1733 (1975).
[17]S. Erhan *et al.*, Phys. Lett. 85B, 447 (1979).
[18]F. Takagi, Report No. TU/82/239 (unpublished); in Proceedings of 13th International Symposium on Multiparticle Dynamics, Volendam, the Netherlands, 1982 (unpublished),
[19]W. Busza, talk presented at 13th International Symposium on Multiparticle Dynamics, Volendam, the Netherlands, 1982 (unpublished).